Institution of
MECHANICAL
ENGINEERS

JOURNAL OF MECHANICAL ENGINEERING SCIENCE

Volume 228 Issue 13
September 2014
ISSN 0954-4062

Proceedings of the Institution of Mechanical Engineers
Part C

http://pic.sagepub.com

Find My Rep | Login | Contact

SAGE Publishing

Search: keyword, title
Search

0

Share

Proceedings of the Institution of Mechanical Engineers, Part C: Journal of Mechanical Engineering Science

2016 Impact Factor: 1.015
2016 Ranking: 91/130 in Engineering, Mechanical
Source: 2016 Journal Citation Reports® (Clarivate Analytics, 2017)

Published in Association with Institution of Mechanical Engineers

Other Titles in:

Engineering & Technology | Mechanical Engineering

eISSN: 20412983 | ISSN: 09544062 | Current volume: 231 | Current issue: 23 Frequency: 18 Times/Year

Download flyer Recommend to Library

- Description
- Aims and Scope
- Editorial Board
- Abstracting / Indexing
- Submission Guidelines

EDITORIAL BOARD

Proceedings of the Institution of Mechanical Engineers, Part C: Journal of Mechanical Engineering Science

Table of Contents

Volume 228, Issue 13, September 2014

Thermodynamics and Heat Transfer

Design and Manufacture

Mechanisms and Machines

Abstract
> Preview

Modeling and analysis of a novel conical magnetic bearing for vernier-gimballing magnetically suspended flywheel

Jiancheng Fang, **Chune Wang**, **Jiqiang Tang**

First Published December 25, 2013; pp. 2416–2425

Abstract
> Preview

Micro- and Nano- Mechanical Systems

Nonlinear analysis of carbon nanotube-based nanoelectronics devices

Mir Masoud Seyyed Fakhrabadi, **Abbas Rastgoo**, **Mohammad Taghi Ahmadian**

First Published January 7, 2014; pp. 2426–2439

Abstract
> Preview

Structural and instrumentation design of a microelectromechanical systems biaxial accelerometer

Ting Zou, **Jorge Angeles**

First Published January 7, 2014; pp. 2440–2455

Abstract
> Preview

Corrigendum

Corrigendum

First Published July 24, 2014; pp. 2456–2456

Abstract
> Preview

RELATED CONTENT

Proceedings of the Institution of Mechanical Engineers, Part C: Journal of Mechanical Engineering Science

ISSN: 0954-4062
Online ISSN: 2041-2983

Proceedings of the Institution of Mechanical Engineers, Part C: Journal of Mechanical Engineering Science
http://pic.sagepub.com/

Collision avoidance control for a human-operated four-wheeled mobile robot

Naoki Uchiyama, Tresna Dewi and Shigenori Sano

Proceedings of the Institution of Mechanical Engineers, Part C: Journal of Mechanical Engineering Science 2014 228: 2278 originally published online 16 January 2014
DOI: 10.1177/0954406213518523

The online version of this article can be found at:
http://pic.sagepub.com/content/228/13/2278

Published by:
SAGE
http://www.sagepublications.com

On behalf of:
Institution of Mechanical Engineers

Original Article

Institution of MECHANICAL ENGINEERS

Journal of MECHANICAL ENGINEERING SCIENCE

Proc IMechE Part C:
J Mechanical Engineering Science
2014, Vol. 228(13) 2278–2284

DOI: 10.1177/0954406213518523
pic.sagepub.com
SAGE

Collision avoidance control for a human-operated four-wheeled mobile robot

Naoki Uchiyama, Tresna Dewi and Shigenori Sano

Abstract

Because the collision avoidance function is indispensable for providing safe and easy operation of human-operated robotic systems, this paper deals with the collision avoidance control for a human-operated mobile robot in unknown environments. A typical four-wheeled mobile robot with infrared distance sensors for detecting obstacles is considered. The robot cannot move in an arbitrary direction owing to a nonholonomic constraint. Therefore, we propose a simple control approach in which a human operator's control input is modified in real time to satisfy the nonholonomic constraint and avoid collision with obstacles. The proposed controller has steering- and brake-like functions that are adjusted according to the distance sensor information. The stability of the proposed control system is analyzed with a linear model. The effectiveness of the proposed method is confirmed by experiments in which several operators control the robot in an environment with obstacles.

Keywords

Four-wheeled mobile robot, collision avoidance, human-operated mobile robot

Date received: 10 June 2013; accepted: 26 November 2013

Introduction

Fully automated robots are desirable to support household chores, nursing and welfare work, and industrial tasks performed by skilled workers. However, from the viewpoint of cost efficiency, it is impractical to produce such robots using the currently available technology. Human-operated robotic systems are a suitable solution, and hence, widely studied. The objectives of human-operated robots include extending human mechanical power,[1,2] providing precise and smooth operations in difficult physical tasks,[3,4] and executing missions in remote or hazardous environments.[5,6] In human-operated robotic systems, controllers are required to incorporate the human operator commands and compensate for operator's mistakes without hampering the ease of operation. Collision avoidance functions are necessary for easy and safe operation of a robot operated by an elderly or disabled person. We consider a collision avoidance control for human-operated four wheeled mobile robots that are widely used in common vehicle systems.

Much research has been conducted on obstacle avoidance for mobile robots.[7–11] The potential field method based on the idea of imaginary forces acting on a robot is one of the most popular approaches to obstacle avoidance. This approach has been extended by many studies. Because the four-wheeled robot is a nonholonomic system, the obstacle avoidance function must consider this dynamic property. The robot manipulator dynamics is considered and decoupled in the implementation of the obstacle avoidance function presented in Ref. 7; however, this decoupling approach cannot be applied to the nonholonomic four-wheeled mobile robot. The dynamic window approach is one of the most efficient approaches that consider the nonholonomic constraint and can be applied to unknown environments.[12,13] In this approach, the mobile robot destination is given and the robot motion is generally determined by

Department of Mechanical Engineering, Toyohashi University of Technology, Toyohashi, Aichi, Japan

Corresponding author:
Naoki Uchiyama, Department of Mechanical Engineering, Toyohashi University of Technology, 1-1 Hibarigaoka, Tempaku, Toyohashi, Aichi 441-8580, Japan.
Email: uchiyama@tut.jp

optimizing a certain cost function such as the distance to the destination.

In the field of autonomous vehicle control, Reichardt and Schick[14] proposed the concept of risk map to achieve human-like behavior. A risk map is an egocentric map of potentials reflecting the risk at a certain position in the environment. Gerdes and Rossetter[15] and Rossetter et al.[16] proposed an approach based on the concept of artificial potential fields, which ensures safe motion in the absence of driver inputs. Wolf and Burdick[17] presented a set of potential function components to assist automated and semiautomated vehicles. However, these approaches require computational effort and expensive sensors to construct and employ the risk map and artificial potential fields. This paper aims to present a simple approach that employs inexpensive distance sensors.

The social force model, which has been used to explain pedestrian motion,[18–20] considers the dynamics of a pedestrian and the imaginary social forces acting on him/her in order to avoid collisions with other people or walls. Based on this concept, we propose a control approach for collision avoidance in which the control input signal is modified according to the distance sensor information. The proposed control system is an extension of that in Ref. 21 to a four-wheeled robot. A stability analysis is performed to validate the proposed approach. The effectiveness of the proposed approach is demonstrated by experimental results obtained when several unskilled operators control the four-wheeled robot in a corridor-like environment.

Controller design for collision avoidance

Social force model

Helbing and Molnar[18] first introduced the social force model to explain pedestrian motion. The social forces are considered to act on a pedestrian in order to avoid collisions with other people or walls and to enable motion in a specific direction at a given speed. The social forces for collision avoidance are modeled as repulsion forces from obstacles such as other people or walls. Follow-up studies on this concept have been conducted.[19,20] This subsection briefly explains the concept of the social force model. The social force model is defined as follows

$$\frac{dw}{dt} = F + F_l \tag{1}$$

where w is the pedestrian velocity vector, F is the social force vector, and F_l is the fluctuation vector. The social force vector F defined in equation (2) consists of the attractive force from the desired position F_α, the repulsive force from other pedestrians and walls F_β, and attractive force from the objects of interest F_γ

$$F = F_\alpha + F_\beta + F_\gamma \tag{2}$$

Helbing and Molnar[18] conducted computer simulations of interacting pedestrians and showed that the social force model can describe the pedestrian behavior including obstacle avoidance. The following section applies this concept to the robot vehicle control.

Dynamics and control of the four-wheeled mobile robot

Figure 1 shows a schematic of the four-wheeled mobile robot. The dynamics of the four-wheeled mobile robot is represented as follows[15]

$$m\dot{u}_x = f_{xr} + f_{xf}\cos\delta - f_{yf}\sin\delta + m\omega u_y \tag{3}$$

$$m\dot{u}_y = f_{yr} + f_{xf}\sin\delta + f_{yf}\cos\delta - m\omega u_x \tag{4}$$

$$I\dot{\omega} = -af_{xf}\sin\delta + af_{yf}\cos\delta - bf_{yr} + \frac{d}{2}\{f_{xrr} - f_{xlr} + (f_{xrf} - f_{xlf})\cos\delta\} \tag{5}$$

$$f_{xf} = f_{xrf} + f_{xlf}, \quad f_{xr} = f_{xrr} + f_{xlr},$$
$$f_{yf} = f_{yrf} + f_{ylf}, \quad f_{yr} = f_{yrr} + f_{ylr}$$

where u_x is the vehicle velocity in front–rear direction; u_y, vehicle velocity in the lateral direction; ω, vehicle angular velocity; f_{ijk}, force acting on each wheel [i: force direction (x or y), j: right(r) or left(l) wheel, k: front(f) or real(r) wheel]; δ, steering angle; m, vehicle mass; a, b, distance between the center of gravity and the rear or front wheel; d, distance between rear wheels (front wheels); and $(\dot{\ })$ is the time derivative.

We assume that f_{xr} and δ are inputs provided by an operator, $f_{xrr} = f_{xlr}$, f_{xrf} and f_{xlf} are zero (i.e. rear-wheel drive), and vehicle parameters m, I, a, b, and d are known and constant. The forces f_{yf} and f_{yr} are approximated as follows[15]

$$f_{yf} \simeq -c_f\gamma_f = -c_f\tan^{-1}\left(\frac{u_y + \omega a}{u_x}\right) - \delta \tag{6}$$

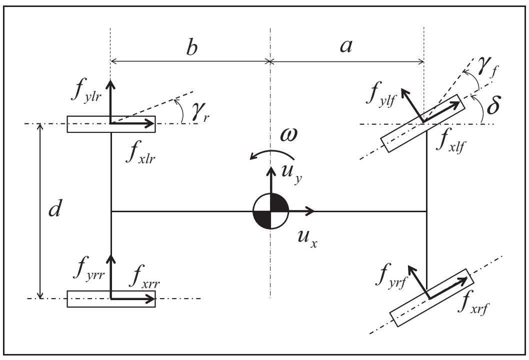

Figure 1. Four-wheeled robot model.

$$f_{yr} \simeq -c_r\gamma_r = -c_r \tan^{-1}\left(\frac{u_y - \omega b}{u_x}\right) \tag{7}$$

where c_f and c_r are the cornering stiffness and γ_f and γ_r are the sliding angles of the front and rear wheels. From equations (3) to (7), we have the following dynamics

$$m\dot{u}_x = f_{xr} + c_f\left\{\tan^{-1}\left(\frac{u_y + \omega a}{u_x}\right) - \delta\right\} \sin\delta + m\omega u_y \tag{8}$$

$$m\dot{u}_y = -c_r \tan^{-1}\left(\frac{u_y - \omega b}{u_x}\right) - c_f\left\{\tan^{-1}\left(\frac{u_y + \omega a}{u_x}\right) - \delta\right\} \cos\delta - m\omega u_x \tag{9}$$

$$I\dot{\omega} = -ac_f\left\{\tan^{-1}\left(\frac{u_y + \omega a}{u_x}\right) - \delta\right\} \cos\delta + bc_r \tan^{-1}\left(\frac{u_y - \omega b}{u_x}\right) \tag{10}$$

This study assumes that several distance sensors are located on the robot. Figure 2 shows an example of a sensor location for the rectangular shaped robot. Because the distance information to obstacles is available, we include this information in steering angles and driving force generated by rear wheels for collision avoidance as follows

$$\delta = \delta_d + \sum_{i=1}^{m} g_{ri} - \sum_{i=1}^{m} g_{li} \tag{11}$$

$$f_{xr} = f_d - \sum_{i=1}^{m} h_{ri} - \sum_{i=1}^{m} h_{li} \tag{12}$$

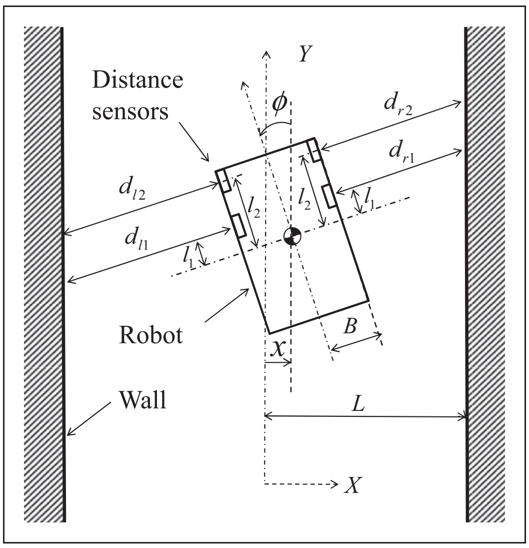

Figure 2. Robot moving between walls.

where δ_d and f_d are the steering angle and driving force designated by an operator, respectively, and f_d corresponds to the accelerating or braking force of a typical vehicle. The virtual steering angles g_{ri} and g_{li} are assumed to be proportional to the distance measurement at each sensor location as follows

$$g_{ki} = -p_i d_{ki} + q_i, \quad k = l, r \tag{13}$$

where the subscript l or r denote that the corresponding sensor is located on the left or right side of the robot body, i the sensor number, and p_i and q_i are positive constants. In this study, g_{ri} and g_{li} are assumed to be positive. Equation (11) indicates that the controller steers to the left when the distance to the obstacle measured by the sensor located at the right-hand side of the robot becomes small and vice versa.

Because we cannot directly apply the social force to the dynamics in equations (3) to (5), we propose to include the similar effect in the steering angle and driving force, as given in equations (11) and (12), which are common control variables in four-wheeled vehicle systems. This controller design has not been presented as far as the author's knowledge.

For simplicity, the virtual forces h_{ri} and h_{li} in equation (12) are assumed to be proportional to the distance measurement at each sensor location as follows

$$h_{ki} = -\hat{p}_i d_{ki} + \hat{q}_i, \quad k = l, r \tag{14}$$

where $\hat{p}_i$ and $\hat{q}_i$ are positive constants. From equation (12), it can be seen that the smaller the distance, the larger the braking force provided by the controller. The effect of g_{ki} and h_{ki} can be interpreted as in the social force model, in which the social force is modeled as a virtual repulsive force to avoid collisions with obstacles.

Stability analysis

Using the test case presented in Figure 2, we consider the validity of the proposed method for realizing the collision avoidance function in the human-operated robot. Namely, this subsection is devoted for analyzing the validity of the control in equations (11) and (12), and the measurement of rotational deviation and forward speed as well as actual parameter values is not required for the control and the analysis in this subsection. Although the vehicle system has nonlinear dynamics in equations (3) to (5), we apply a linear analysis at a certain operating point that is generally effective to predict the fundamental property of the control system. Experiments were conducted to further verify the effectiveness, and their results are shown in "Experiments" section. For simplicity, the robot is assumed to have a rectangular shape. It is further assumed that the human operator intends to move the robot along the centerline between two parallel walls. Because of operational mistakes, the robot deviates from the centerline as shown in Figure 2. The lateral and rotational deviations are denoted by x and ϕ, respectively. The position in the vertical direction is denoted by y. In addition, we assume that all distance sensors are located symmetrically with respect to the centerline and only above the robot's center of gravity, as shown in the figure. The number of sensors located at the left or right half side of the robot is denoted by N.

The distance between each sensor and the walls is given as follows

$$d_{ri} = \frac{L-x}{\cos\phi} + l_i \tan\phi - B \tag{15}$$

$$d_{li} = \frac{L+x}{\cos\phi} - l_i \tan\phi - B \tag{16}$$

where L is the half distance between the walls and B is the half width of the robot. l_i is the distance from the robot's center of gravity to the ith distance sensor along the robot's center line.

From Figure 2, we obtain the following relations

$$\dot{x} = -u_x \sin\phi - u_y \cos\phi \tag{17}$$

$$\dot{y} = u_x \cos\phi - u_y \sin\phi \tag{18}$$

$$\dot{\phi} = \omega \tag{19}$$

Assuming that the robot moves with approximately the constant speed (operating point) $(u_x, u_y, \omega) = (u_{x0}, 0, 0)$ as follows

$$u_x = u_{x0} + u_{xs}, \quad u_y = u_{ys}, \quad \omega = \omega_s \tag{20}$$

where $(u_{xs},\ u_{ys},\ \omega_s)$ is the deviation from the operating point and the steering angle δ is small. Linearizing equations (8) to (10), we obtain the following linearized dynamics

$$m\dot{u}_{xs} = f_{xr} \tag{21}$$

$$m\dot{u}_{ys} = -c_r \frac{u_{ys} - b\omega_s}{u_{x0}} - c_f \frac{u_{ys} + a\omega_s}{u_{x0}} + c_f \delta - m\omega_s u_{x0} \tag{22}$$

$$I\dot{\omega}_s = -ac_f \frac{u_{ys} + a\omega_s}{u_{x0}} + ac_f\delta + bc_r \frac{u_{ys} - b\omega_s}{u_{x0}} \tag{23}$$

Furthermore, assuming that the angle ϕ is small and substituting equations (17) to (19) after linearization, controller equations (11) and (12), and distance equations (15) and (16) into equations (21) to (23) yields the following dynamics

$$\ddot{y} = \frac{f_{xr}}{m} \tag{24}$$

$$\ddot{x} = -\frac{c_r + c_f}{mu_{x0}}\dot{x} - \frac{2c_f \sum_{i=1}^{N} p_i l_i}{m} x + \left(u_{x0} - \frac{bc_r - ac_f}{mu_{x0}}\right)\dot{\phi} + \frac{2c_f \sum_{i=1}^{N} p_i l_i}{m}\phi \tag{25}$$

$$\ddot{\phi} = -\frac{ac_f - bc_r}{Iu_{x0}}\dot{x} - \frac{2ac_f \sum_{i=1}^{N} p_i l_i}{I} x - \frac{a^2 c_f + b^2 c_r}{Iu_{x0}}\dot{\phi} - \frac{2ac_f \sum_{i=1}^{N} p_i l_i}{I}\phi \tag{26}$$

where we assume the desired steering angle $\delta_d = 0$. The breaking force effect appears as in equation (24), and it is obvious that the motion is decelerated when f_{xr} is negative. Because the control objective is to reduce the deviation in the x and ϕ directions, we only consider equations (25) and (26) for the stability analysis. It should be noted that owing to the nonholonomic constraint, the robot cannot move instantaneously in the x direction. Hence, we only consider the ϕ dynamics in equation (26) for the stability analysis.

To validate the proposed method, we simply consider the case that the vehicle's front and rear sides and the cornering stiffness satisfy $a \simeq b$ and $c_f \simeq c_r$, respectively. Then, we can rewrite equation (26) as follows

$$\ddot{\phi} + c_1\dot{\phi} + c_2\phi = c_3 x \tag{27}$$

where $c_1 \sim c_3$ are positive constants. Equation (27) is a stable system with respect to ϕ. In addition, the positive value of x provides a positive steady-state value for ϕ, which makes the robot turn left and reduces the magnitude of x. Similarly, when x has a negative value, the negative steady-state value for ϕ causes the robot to turn right and reduces the magnitude of x. Hence, this approach is expected to provide the appropriate collision avoidance function.

Experiments

Figure 3 shows the experimental robot equipped with distance sensors and the controller for human operators. The measurable range of the distance sensor is 10–80 cm. Rotary encoders (500 PPR) attached to the motors are used for measuring the robot position and orientation by assuming that the wheel slip is negligible. The proposed controller design is verified in the environment shown in Figure 4, where the robot controlled by six operators is expected to move from the start position to the destination.

In order to achieve the effective collision avoidance, it is reasonable to employ a function that provides a larger steering angle and breaking force near obstacles compared with equations (13) and (14).

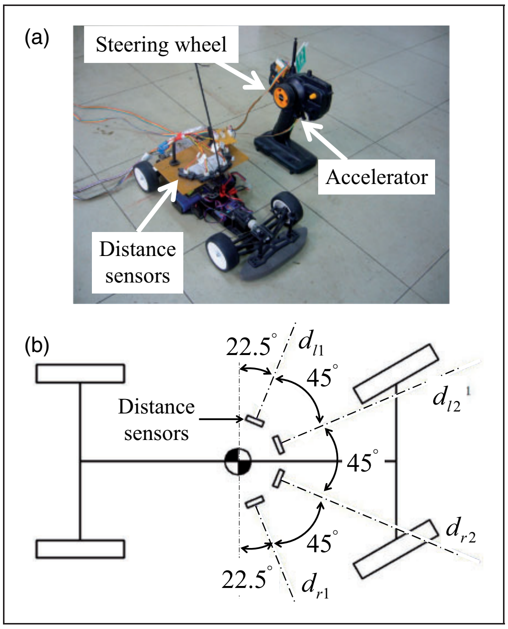

Figure 3. Experimental robot system.

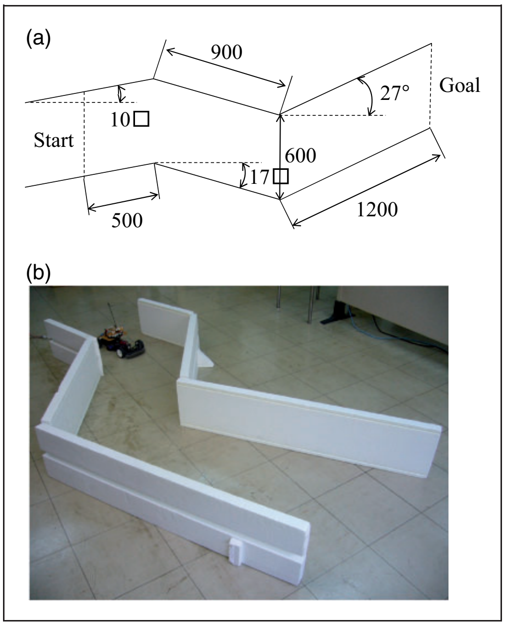

Figure 4. Experimental environment.

We consider the following nonlinear functions instead of equations (13) and (14)

$$g_{ki} = \frac{\alpha_i}{\sqrt[n]{d_{ki}}}, \quad k = l, r \tag{28}$$

$$h_{ki} = \frac{\beta_i}{\sqrt[n]{d_{ki}}}, \quad k = l, r \tag{29}$$

Figure 5 shows the profile of these functions in which the parameters are set as $\alpha_i = 0.5$ and $n = 1,\ 2,\ 5$. Regarding to the stability analysis, linearizing equations (28) and (29) leads to equations (13) and (14), and hence the linear analysis assuming a certain operating point in "Stability analysis" section is still valid for linearized equations of (28) and (29). Table 1 lists the parameters used in the experiment. Each operator operates the robot under the following conditions:

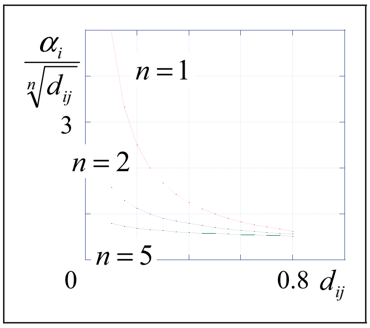

Figure 5. Function profile used for collision avoidance.

Table 1. Experimental parameters.

Parameter	Value	Parameter	Value
m	1.33 (kg·m^2)	α_1	2.0×10^{-3} (rad·m$^{1/3}$)
I	0.02 (kg·m^2)	α_2	4.6×10^{-3} (rad·m$^{1/3}$)
a	0.09 (m)	β_1	0.4 (N·m$^{1/3}$)
b	0.07 (m)	β_2	0.5 (N·m$^{1/3}$)
C_f	15.0 (N/rad)	n	3
C_r	15.0 (N/rad)		

Table 2. Number of collisions occurred for each operator.

Operator No.	Manual	Proposed
1	3	0
2	2	0
3	1	0
4	3	0
5	1	0
6	2	0

1. Without the collision avoidance function (if the robot collides with the wall, the operator operates the robot from the start position again).
2. With the collision avoidance function.

In case 2, we consider the worst case that the operator can control only on/off of the translational motion, and the breaking and the steering are controlled automatically.

Table 2 presents the number of collisions for each operator. No collisions occurred while operating the robot with the collision avoidance function.

Figure 6 compares the time required for each operator to reach the goal. Because the robot collided the

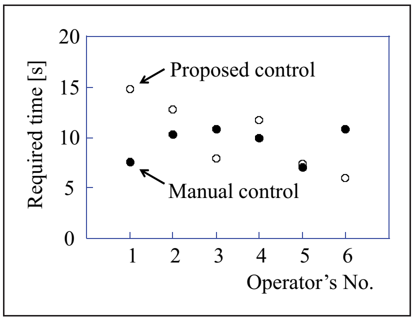

Figure 6. Comparison of required time to reach the goal.

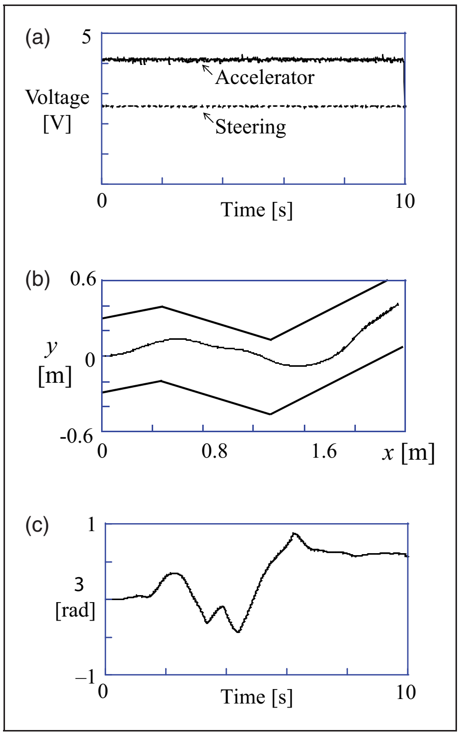

Figure 7. Proposed control results. (a) Commanded control input voltage, (b) robot position, and (c) robot orientation.

wall during the trial of all operators, they performed several trials and the required time was reduced in the last trial. The figure shows the required time recorded in the last trial of the manual control case. On an average, there is no significant difference in the required time to reach the goal with and without the proposed method. The average times were 9.42 s for the manual control case and 10.12 s for the proposed method.

Figures 7 and 8 compare the operator control with and without the proposed method. Figures 7(a) and 8(a) show the control input voltage commanded by the operator. The control input voltage has the following relation to the steering angle δ_d and acceleration force f_d in equations (11) and (12), respectively

$$\delta_d = \frac{\pi}{180} \times \{16.2 \times (V_\delta - V_0)\} \text{ [rad]} \tag{30}$$

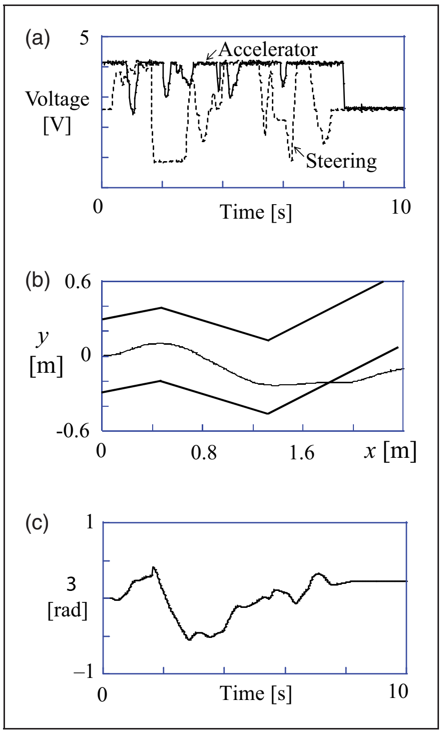

Figure 8. Manual control results. (a) Commanded control input voltage, (b) robot position, and (c) robot orientation.

$$f_d = 0.23 \times (V_f - V_0) \text{ [N]} \tag{31}$$

where V_δ and V_f are control input voltages commanded by the human operators and $V_0 = 2.65$ V. In Figure 7, although the operator does not steer the robot, it successfully moves to the goal by automatically adjusting the steering angle ϕ. In Figure 8, the operator frequently adjusts both the steering wheel and accelerator. However, a collision occurs at approximately $x = 1.8$ m in Figure 8(b). These results confirm the effectiveness of the proposed controller design using inexpensive distance sensors and simple control input calculations.

Experimental results show that the proposed control in equations (11) and (12) can provide successful collision avoidance for the worst case that the operator can control only on/off of the translational motion. For the case that the operator can control the speed and the steering, the effect of functions g_{ki} and h_{ki} in equations (11) and (12) may be tuned by changing the values α_i and n in Figure 5. If the operator is skillful, the effect should be reduced, otherwise, it should be increased. Hence, the proposed control may be useful for any level of operators in collision avoidance.

Conclusions

This paper presents a new approach to collision avoidance for four-wheeled human-operated mobile robots using inexpensive infrared distance sensors.

Because the proposed method considers the nonholonomic constraint of a mobile robot, it provides practical collision avoidance control. The effectiveness of the proposed approach is demonstrated by the results of the experiment, in which all unskilled operators could maneuver the robot to the destination without collisions. In future studies, the presented linear analysis will be extended to more general cases and the proposed robot system will be applied to more complex environments.

Funding

This research received no specific grant from any funding agency in the public, commercial, or not-for-profit sectors.

References

1. Kazerooni H. Human-robot interaction via the transfer of power and information signals. *IEEE Trans Syst Man Cybernet* 1990; 20: 450–463.
2. Kazerooni H and Steger R. The Berkeley lower extremity exoskeleton. *ASME J Dyn Syst Meas Control* 2006; 128: 14–25.
3. Peshkin MA, Colgate JE, Wannasuphoprasit W, et al. Cobot architecture. *IEEE Trans Robot Automat* 2001; 17: 377–390.
4. Bettini A, Marayong P, Lang S, et al. Vision-assisted control for manipulation using virtual fixtures. *IEEE Trans Robot Automat* 2001; 20: 953–966.
5. Anderson RJ and Spong MW. Bilateral control of teleoperators with time delay. *IEEE Trans Automat Control* 1989; 34: 494–501.
6. Lawrence DA. Stability and transparency in bilateral teleoperation. *IEEE Trans Robot Automat* 1993; 9: 624–637.
7. Khatib O. Real-time obstacle avoidance for manipulators and mobile robots. *Int J Robot Res* 1986; 5: 90–98.
8. Latombe JC. *Robot motion planning*. Norwell, MA: Kluwer Academic Publishers, 1991.
9. Chakravarthy A and Ghose D. Obstacle avoidance in a dynamic environment: A collision cone approach. *IEEE Trans Syst Man Cybernet Part A Syst Humans* 1998; 28: 562–574.
10. Borenstein J and Koren Y. Real-time obstacle avoidance for fast mobile robots. *IEEE Trans Syst Man Cybernet* 1989; 19: 1179–1187.
11. Lamiraux F, Bonnafous D and Lefebvre O. Reactive path deformation for nonholonomic mobile robots. *IEEE Trans Robot Automat* 2004; 20: 967–977.
12. Fox D, Burgard W and Thrun S. The dynamic window approach to collision avoidance. *IEEE Robot Automat Mag* 1997; 4: 22–23.
13. Ögren P and Leonard NE. A convergent dynamic window approach to obstacle avoidance. *IEEE Trans Robot Automat* 2005; 21: 188–195.
14. Reichardt D and Schick J. Collision avoidance in dynamic environments applied to autonomous vehicle guidance on the motorway. In: *Proceedings of the intelligent vehicles symposium*, Paris, France, 1994, pp.74–78.
15. Gerdes JC and Rossetter EJ. A unified approach to driver assistance systems based on artificial potential fields. *Trans ASME J Dyn Syst Meas Control* 2001; 123: 431–438.
16. Rossetter EJ, Switkes JP and Gerdes JC. Experimental validation of the potential field driver assistance system. *Int J Automot Technol* 2004; 5: 95–108.
17. Wolf MT and Burdick JW. Artificial potential functions for highway driving with collision avoidance. In: *Proceedings of IEEE international conference on robotics and automation*, Pasadena, CA, 2008, pp.3731–3736.
18. Helbing D and Molnar P. Social force model for pedestrian dynamics. *Phys Rev* 1995; E51: 4282–4286.
19. Lakoba TI and Kaup DJ. Modification of the Helbing-Molnar-Farkas-Vicsek social force model for pedestrian evolution. *Simulation* 2005; 81: 339–352.
20. Helbing D, Farkas I and Vicsek T. Simulating dynamical features of escape panic. *Nature* 2000; 407: 487–490.
21. Uchiyama N, Hashimoto T, Sano S, et al. Model-reference control approach to obstacle avoidance for a human-operated mobile robot. *IEEE Trans Ind Electron* 2009; 56: 3892–3896.